

Towards fast femtosecond laser micromachining of fused silica: The effect of deposited energy.

Sheeba Rajesh and Yves Bellouard

Micro- & Nano- Scale Engineering, Mechanical Engineering Department, Eindhoven University of Technology, P.O. Box 513, 5600 MB, Eindhoven, The Netherlands.
y.bellouard@tue.nl

Abstract: Femtosecond laser micromachining of glass material using low-energy, sub-ablation threshold pulses find numerous applications in the fields of integrated optics, lab-on-a-chips and microsystems in general. In this paper, we study the influence of the laser-deposited energy on the performance of the micromachining process. In particular, we show that the energy deposited in the substrate affects its etching rate. Furthermore, we demonstrate the existence of an optimal energy deposition value. These results are not only important from an industrial point-of-view but also provide new evidences supporting the essential role of densification and consequently stress-generation as the main driving factor promoting enhanced etching rate following laser exposure.

©2010 Optical Society of America

OCIS codes: (140.7090) Ultrafast lasers; (160.2750) Glass and other amorphous materials; (320.2250) femtosecond phenomena; (320.7130) Ultrafast processes in condensed matter, including semiconductors.

References and links

1. K. M. Davis, K. Miura, N. Sugimoto, and K. Hirao, "Writing waveguides in glass with a femtosecond laser," *Opt. Lett.* **21**(21), 1729–1731 (1996).
2. Y. Sikorski, A. Said, P. Bado, R. Maynard, C. Florea, and K. Winick, "Optical waveguide amplifier in Nd-doped glass written with near-IR femtosecond laser pulses," *Electron. Lett.* **36**(3), 226–227 (2000).
3. K. Minoshima, A. M. Kowalevicz, I. Hartl, E. P. Ippen, and J. G. Fujimoto, "Photonic device fabrication in glass by use of nonlinear materials processing with a femtosecond laser oscillator," *Opt. Lett.* **26**(19), 1516–1518 (2001).
4. S. Nolte, M. Will, J. Burghoff, and A. Tuennermann, "Femtosecond waveguide writing: a new avenue to three-dimensional integrated optics," *Appl. Phys., A Mater. Sci. Process.* **77**(1), 109–111 (2003).
5. R. Osellame, S. Taccheo, M. Marangoni, R. Ramponi, P. Laporta, D. Polli, S. De Silvestri, and G. Cerullo, "Femtosecond writing of active optical waveguides with astigmatically shaped beams," *J. Opt. Soc. Am. B* **20**(7), 1559–1567 (2003).
6. R. W. A. Applegate, Jr., J. Squier, T. Vestad, J. Oakey, D. W. M. Marr, P. Bado, M. A. Dugan, and A. A. Said, "Microfluidic sorting system based on optical waveguide integration and diode laser bar trapping," *Lab Chip* **6**(3), 422–426 (2006).
7. Y. Hanada, K. Sugioka, H. Kawano, I. S. Ishikawa, A. Miyawaki, and K. Midorikawa, "Nano-aquarium for dynamic observation of living cells fabricated by femtosecond laser direct writing of photostructurable glass," *Biomed. Microdevices* **10**(3), 403–410 (2008).
8. Y. Bellouard, A. Said, and P. Bado, "Integrating optics and micro-mechanics in a single substrate: a step toward monolithic integration in fused silica," *Opt. Express* **13**(17), 6635–6644 (2005), <http://www.opticsinfobase.org/oe/abstract.cfm?URI=oe-13-17-6635>.
9. Y. Bellouard, A. Said, M. Dugan, and P. Bado, "Monolithic integration in fused silica: When fluidics, mechanics and optics meet in a single substrate," in *International Symposium on Optomechatronic Technologies* (2009), pp. 445–450.
10. A. Marcinkevi Ius, S. Juodkazis, M. Watanabe, M. Miwa, S. Matsuo, H. Misawa, and J. Nishii, "Femtosecond laser-assisted three-dimensional microfabrication in silica," *Opt. Lett.* **26**(5), 277–279 (2001).
11. Y. Bellouard, A. Said, M. Dugan, and P. Bado, "Fabrication of high-aspect ratio, micro-fluidic channels and tunnels using femtosecond laser pulses and chemical etching," *Opt. Express* **12**(10), 2120–2129 (2004), <http://www.opticsinfobase.org/oe/abstract.cfm?URI=oe-12-10-2120>.
12. S. Kiyama, S. Matsuo, S. Hashimoto, and Y. Morihira, "Examination of Etching Agent and Etching Mechanism on Femtosecond Laser Microfabrication of Channels Inside Vitreous Silica Substrates," *J. Phys. Chem. C* **113**(27), 11560–11566 (2009).

13. C. Hnatovsky, R. S. Taylor, E. Simova, V. R. Bhardwaj, D. M. Rayner, and P. B. Corkum, "Polarization-selective etching in femtosecond laser-assisted microfluidic channel fabrication in fused silica," *Opt. Lett.* **30**(14), 1867–1869 (2005).
14. C. Schaffer, J. García, and E. Mazur, "Bulk heating of transparent materials using a high-repetition-rate femtosecond laser," *Appl. Phys., A Mater. Sci. Process.* **76**(3), 351–354 (2003).
15. S. Eaton, H. Zhang, P. Herman, F. Yoshino, L. Shah, J. Bovatsek, and A. Arai, "Heat accumulation effects in femtosecond laser-written waveguides with variable repetition rate," *Opt. Express* **13**(12), 4708–4716 (2005), <http://www.opticsinfobase.org/oe/abstract.cfm?URI=oe-13-12-4708>.
16. W. Yang, P. G. Kazansky, Y. Shimotsuma, M. Sakakura, K. Miura, and K. Hirao, "Ultrashort-pulse laser calligraphy," *Appl. Phys. Lett.* **93**(17), 171109 (2008).
17. W. Yang, P. G. Kazansky, and Y. P. Svirko, "Non-reciprocal ultrafast laser writing," *Nat. Photonics* **2**(2), 99–104 (2008).
18. B. Poumellec, M. Lancry, J.-C. Poulain, and S. Ani-Joseph, "Non reciprocal writing and chirality in femtosecond laser irradiated silica," *Opt. Express* **16**(22), 18354–18361 (2008), <http://www.opticsinfobase.org/abstract.cfm?URI=oe-16-22-18354>.
19. J. W. Chan, T. Huser, S. Risbud, and D. M. Krol, "Structural changes in fused silica after exposure to focused femtosecond laser pulses," *Opt. Lett.* **26**(21), 1726–1728 (2001).
20. Y. Bellouard, E. Barthel, A. A. Said, M. Dugan, and P. Bado, "Scanning thermal microscopy and Raman analysis of bulk fused silica exposed to low-energy femtosecond laser pulses," *Opt. Express* **16**(24), 19520–19534 (2008), <http://www.opticsinfobase.org/oe/abstract.cfm?URI=oe-16-24-19520>.
21. Y. Bellouard, T. Colomb, C. Depeursinge, M. Dugan, A. A. Said, and P. Bado, "Nanoindentation and birefringence measurements on fused silica specimen exposed to low-energy femtosecond pulses," *Opt. Express* **14**(18), 8360–8366 (2006), <http://www.opticsinfobase.org/oe/abstract.cfm?URI=oe-14-18-8360>.
22. M. Tomozawa, Y. Lee, and Y. Peng, "Effect of uniaxial stresses on silica glass structure investigated by IR spectroscopy," *J. Non-Cryst. Solids* **242**(2-3), 104–109 (1998).
23. A. Agarwal, and M. Tomozawa, "Correlation of silica glass properties with the infrared spectra," *J. Non-Cryst. Solids* **209**(1-2), 166–174 (1997).
24. Y. Shimotsuma, P. G. Kazansky, J. Qiu, and K. Hirao, "Self-organized nanogratings in glass irradiated by ultrashort light pulses," *Phys. Rev. Lett.* **91**(24), 247405 (2003).
25. K. Awazu, and H. Kawazoe, "Strained Si–O–Si bonds in amorphous SiO₂ materials: A family member of active centers in radio, photo, and chemical responses," *J. Appl. Phys.* **94**(10), 6243–6262 (2003).

1. Introduction: femtosecond laser process combined with chemical etching

Femtosecond laser processing with low-energy pulses eventually combined with chemical etching of dielectrics is finding numerous promising applications not only for integrated optics (see for instance [1–5]) but also for lab-on-a-chip (see for instance [6,7]) and more generally for highly integrated three-dimensional monolithic microsystems [8] that combine optical, fluid-handling and mechanical functions in a single substrate [9]. Although various substrates have been considered (for instance photo-etchable glass [7]), fused silica (the glassy phase of SiO₂) offers the most attractive properties such as low self-fluorescence, high chemical stability and a broad transmission spectrum.

The process of femtosecond laser exposure combined with etching - first reported by Markincevicius *et al.* [10] for fused silica - involves two steps that are depicted in Fig. 1. First, the substrate is exposed to a tightly focused femtosecond laser-beam emitting low-energy pulses, typically below or in the range of 1μJ. Patterns are 'written' by moving the specimen under the laser beam (for instance using motorized stages). The pulse energy levels are such that no material is removed but structural modifications of the material take place at the laser focal spot. The process for making any arbitrary shape is further described in [11].

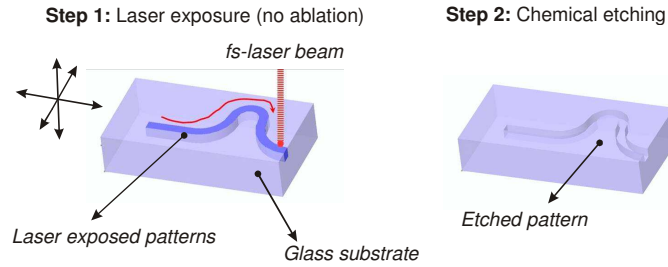


Fig. 1. Illustration of the femtosecond laser processing combined with chemical etching. In a first step, the material is exposed to the laser beam. Low energy pulses are typically used. No ablation is performed; rather the internal structure of the material is modified. In a second step, the exposed patterns are revealed by dipping the glass specimen in a chemical etching bath.

Second, preferential chemical etching of the laser-processed region is performed by immersing the substrate in an etching agent. Low-concentration HF (typ. Less than 10%) is generally used and leads to aspect ratio of about 1:20 to 1:50 depending on the etchant concentration. Interestingly, it was recently shown by Kiyama *et al.* [12] that heated-KOH might offer significantly better aspect ratio (the authors reported 1:200) without significant saturation behavior as observed with HF. For both etchants, HF [13] and KOH [12], the etching rate strongly depends on the polarization state of the laser beam used to write the patterns.

In this paper, we study the role of the deposited energy (or ‘net fluence’) on the etching process of femtosecond laser exposed fused silica specimens.

2. Methods

2.1 Estimation of the deposited energy

A simple way to define an amount of deposited energy is to consider how much energy is passing through a given surface element equal to the spot area in the waist plane. Figure 2 illustrates the concept of deposited energy.

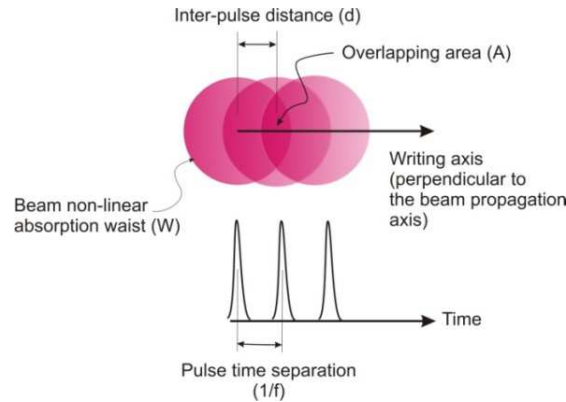


Fig. 2. Cut-view diagram showing the overlap of laser pulses non-linear absorption waists as the beam is moved along at a speed v . The frequency at which the pulses are emitted is f .

The effective number of pulses delivered in a surface corresponding to the non-linear absorption beam diameter can be written as:

$$M = \frac{w_{nla} f}{v}, \quad (1.1)$$

where w_{nla} is the non-linear absorption beam waist, f is the laser repetition rate and v is the writing speed. Note that w_{nla} by definition is always smaller or equal to the beam waist.

If we assume that the ratio v/f is much smaller than the non-linear beam waist (in other words that $v/f \ll w_{nla}$), the deposited energy per unit surface Φ_d (or ‘net fluence’) on the specimen can be approximated by:

$$\Phi_d = \frac{4E_p}{\pi w_{nla}^2} M = \frac{4E_p}{\pi w_{nla}} \left(\frac{f}{v} \right), \quad (1.2)$$

in which E_p is the energy deposited for a single pulse. The hypothesis that $v/f \ll w_{nla}$ is a fair assumption considering our experimental conditions. Note that w_{nla} is dependent on the pulse energy as can be clearly seen from scanning thermal microscopy of laser-affected zones [20]. In these experiments, w_{nla} is measured using SEM and optical observations of lines written close to the surface.

In the following paragraph, we analyze the effect of deposited energy for various ratios of M numbers. From (1.2), for a given of deposited energy, an infinite number of couples of values, f and v, can be chosen. The constraints on these two parameters will be set by the laser setup used, that is to say the available repetition rates of the laser and the performance of the specimen positioning device.

From the literature on cumulative effects in waveguide writings [14,15], one can distinguish two regimes. For pulse frequency f below a critical value – that we call here f_c , there is no ‘dynamic’ effect from one pulse to the next one – in other words, in that regime, the frequency at which pulses are delivered does not affect the end results. Above this critical value, dynamic accumulation effects of thermal origin are observed and a cumulative regime is observed. An order of magnitude for the transition between cumulative and non-cumulative regimes (f_c) is 1 to a few MHz.

Here, we explore the non-cumulative regime for various values of f and v and we specifically investigate the role of the deposited energy on the etching efficiency. Pulse energies are chosen below the ablation threshold.

2. Experimental methods

We use a diode-pumped Ytterbium-KGW based femtosecond oscillator (t-Pulse 500 from Amplitude Systèmes) delivering 500fs pulses at 1024nm. The oscillator emits pulses at a frequency of 9.4 MHz. We use an AOM-based setup to lower the repetition rate by chopping off pulses from the main pulse train. This setup allows us to continuously sweep the repetition rate from 0 to 870 kHz without modifying the pulse temporal and energy characteristics. The laser beam is focused inside the specimen using a 20X objective (OFR-20X-1054) optimized for YAG wavelength and with an effective numerical aperture (NA) of 0.40.

The specimens used are cuboids of OH-rich fused silica (Heraeus, Spectrosil, OH = 1000ppm) that are moved under the laser beam using commercial positioning stages (Physik Instruments). Laser writing is performed perpendicularly to the laser beam propagation direction at velocities varying from 0.01mm/s to 35 mm/s. Line patterns are written at a depth of 100 μ m from the surface.

It has been shown that laser polarization affects the chemical etching regime [13]. To take into account these effects, we considered two linear laser polarizations: longitudinal and transverse to the laser writing direction. Recent observations reported in the literature [16–18] indicate that the morphologies of laser-exposed patterns may depend also on the writing direction, possibly due to a pulse-front tilt effect [16]. As a precaution, and for consistency in our analysis, lines were therefore always written in the same direction.

After laser exposure, the specimen were lapped and polished on both ends of the laser-written track to directly expose the laser patterns to the chemical etchant. To suppress surface in-homogeneities at the specimen edges (for instance due to the clipping of the laser beam when the beam reaches the specimen edges as well as possible residual stress from the initial specimen preparation), several tens of microns were removed from both sides.

Prior to etching, specimens are cleaned respectively in isopropanol and acetone solutions in an ultrasonic bath. The cleaned specimens are then immersed in a 2.5% HF etching bath, first for 4 minutes to reveal the laser etched laser patterns and do some scanning electron microscope analysis and then, for four continuous hours to investigate the etching rates.

Three sets of laser lines with the same parameters were written in the specimen at different places to verify the reproducibility of the results. Etching length measurements were done for each line by observing the length of the removed material from both end of the specimen. For this observation, we use optical observations under cross-polarized light to increase the contrast between etched and non-etched zones.

3. Results

Figure 3 shows a log-log plot of writing speed (v) versus deposited energy (E_d) according to Eq. (1) for five repetition rates 100 kHz, 250 kHz, 500 kHz, 860 kHz and 9.4 MHz. The points shown in the graph are experimental data for which we could see visible patterns with an optical microscope. Our setup does not allow us to explore the regime between 860 kHz and 9.4 MHz, therefore the transition between cumulative and non-cumulative regime could not be identified accurately in these experiments. We assume that this transition is around a few MHz as reported by others [14,15]. In the lower repetition rate regime (860 kHz and below), for a given energy deposited level obtained with various combinations of repetition rate and speed, we observe the same visible patterns in the material. In this non-cumulative frequency regime, the rate at which the energy is deposited, have no noticeable influence on the patterns produced.

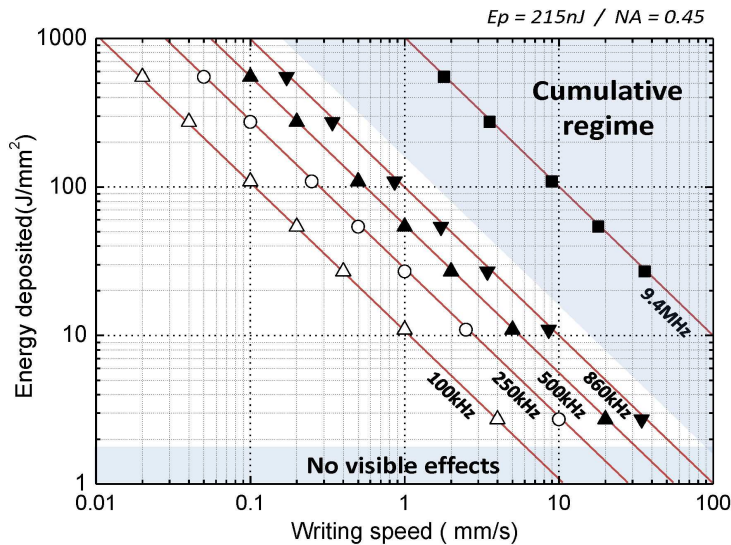


Fig. 3. Log-log plot of the deposited energy (net fluence) versus writing speed. Each point indicates actual measurements for various repetition rates. The pulse energy was kept the same for all experiments.

Figure 4 shows typical optical microscopic observations of partially etched laser tracks for increasing deposited energy levels (from left to right in the figure) and for two repetition rates: 860 kHz and 500 kHz. The etching time was 4 hours in a 2.5% HF acid solution.

The etched portions are easily identifiable thanks to their dark appearance, in sharp contrast with the non-etched zones that appears almost transparent. Figure 5 plots the measured etched lengths for four different repetition rates. For every data points, the laser polarization was set perpendicular to the writing direction and the writing direction was the same. The maximum possible error in the measurement of etched length is $\pm 10 \mu\text{m}$.

Figure 4 clearly shows that the etching length increases with the level of deposited energy and reaches a maximum point followed by a sharp decrease and saturation regime. As shown in Fig. 5, this behaviour is the same for all the laser repetition rates considered in these experiments (from 100 kHz to 860 kHz). In term of etching rate, the maximum corresponds to about 70 microns/h down to an etching rate between 26 to 40 microns/h for the highest levels of deposited energy.

This result emphasizes that, for a given pulse energy, there is an optimal deposited energy to achieve the maximum etching speed and this, independently of the laser repetition rate or, in other words, independently on how fast the energy is deposited in the material. We also observed a similar behaviour for a polarization longitudinal to the writing direction. There, the etched length is typically six times shorter than the perpendicular-to-the-writing-direction polarization case. The effect of laser polarization on etching rate is known and was reported earlier [13]. Here, we observe that the existence of an optimal level of deposited energy is also independent of the laser polarization.

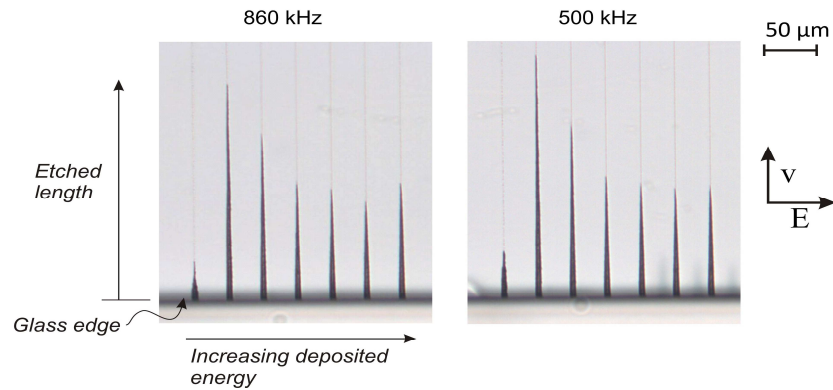


Fig. 4. Optical microscopy image of partially etched laser tracks for increasing deposited energy levels from 2.7 J/mm^2 for the left-most laser line up to 550 J/mm^2 for the right most line. As indicated in the figure, the laser polarization is perpendicular to the writing direction. Lines were written always in the same direction. The pulse energy was 215 nJ.

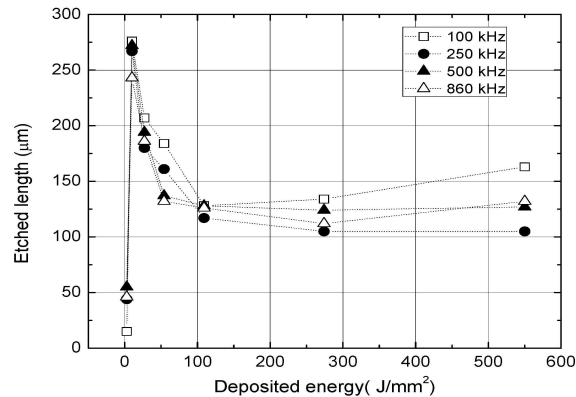


Fig. 5. Deposited energy versus etched length for various repetition rates as measured in an optical microscope. The laser polarization is transverse to the writing direction. The pulse energy (E_p) is 215 nJ. The specimen was etched for 4 hours in a 2.5% HF acid. Measurement errors are estimated to be ± 10 microns for all points.

To examine the morphological details of the laser affected zones, we partially etched the specimen for 4 minutes in 2.5% HF acid bath (this was done prior to etching for four hours for measuring the etched lengths). Figure 6 shows four SEM images (taken in BSE mode) of

partially etched laser lines corresponding to two extreme deposited energies 10 J/mm^2 and 550 J/mm^2 and two polarizations (transverse and longitudinal to the writing direction).

While there are obvious differences of morphology between the two polarizations (as one would expect), for a given polarization, no significant differences could be observed for the two extreme deposited energy levels. For the transverse polarization, we observe very narrow etched trenches suggesting the presence of self-organized nanoscale patterns [24] preferentially etched after 4 minutes.

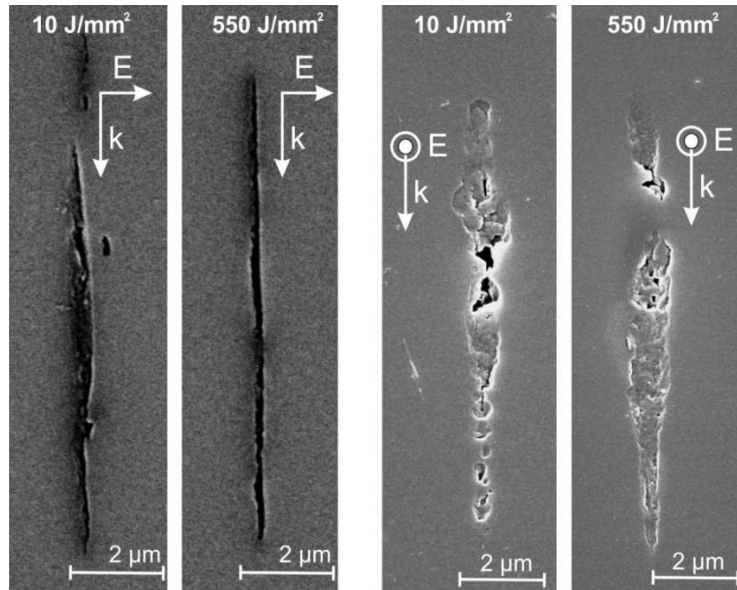


Fig. 6. SEM images (in BSE mode) of partially etched laser lines. The laser was propagating from the top to the bottom of the image. The writing directions were perpendicular to the image plane. The two left images correspond to a transverse polarization (with respect to the writing direction) and to energy deposited levels respectively of 10 J/mm^2 and 550 J/mm^2 . The two right images correspond to a longitudinal polarization (with respect to the writing direction) and to energy deposited levels respectively of 10 J/mm^2 and 550 J/mm^2 . The pulse energy was 215 nJ.

4. Interpretation and hypotheses

From our experiments, we note that even though the laser repetition rate is below the threshold for cumulative effects (typically estimated around 1 MHz), the amount of deposited energy per unit surface affects the HF etching rate of the laser processed material. In particular, we observe an optimum deposited energy level to achieve the fastest etching rate and this, independently on how fast the energy is deposited, i.e. independently to the repetition rate. This suggests that the material response, in terms of structural modifications, gradually evolves with the deposited energy, independently to the time separating two pulses. The etching rate response as a function of deposited energy presents two regimes. First, a sharp increase of the etching rate up to a maximum value, followed by a fast decrease of the etching rate down to a kind of saturation value.

To explain this behavior, we propose the following mechanism. Each single pulse induces structural modifications in the material. These structural modifications can be of various kinds: defects but also formation of smaller SiO_4 -ring structures (as suggested by Raman observations [19,20]) that lead to a gradual densification effect. The hypothesis of laser-induced densification is supported by nano-indentations experiments [21]. If a localized densification take place in a confined and well defined region (as suggested by experimental evidences presented in [11] and [20]), the region surrounding will be put under tensile stress

in order to accommodate the local change of volume. In [21], we reported the presence of stress-induced birefringence surrounding laser written lines.

As the number of pulses impacting the material increases, the material is progressively further densified and, as a consequence, the stress around the laser affected zones builds up. On the other hand, tensile stress also changes the bond angles between the tetrahedral constituents of the SiO₂ matrix [22] [25], which in turn has been correlated to an increase of the HF etching rate of SiO₂ [23]. The higher the tensile stress, the higher the etching rate.

We make the hypothesis that two etching mechanisms are present. One is due to the structural changes observed in the laser-affected zones. The presence of lower order ring structures in the laser-affected zone will enhance the etching rate. The second etching rate enhancement mechanism is due to the tensile stress resulting from the confined densification of the material.

When working with a moderate NA (typically around 0.45) laser affected zones have elliptical shapes for low-energy pulses (see [20]). If these zones are put under uniform stress (due to the densification) high stress concentration areas will be found at the tip of the ellipses. However, when the stress becomes locally too high, a crack will eventually nucleate and propagate through the high-stress zone. The formation of a crack, consumes part of the stored elastic energy, and relaxes the stress in the area surrounding the laser affected zone, thus attenuating the stress-induced enhancement effect. This stress relaxation effect could account for the sudden drop of etching rate (Fig. 5).

As observed in Fig. 5, the etching rate does not drop to zero but saturate around some smaller and relatively constant value. This fact suggests that the enhanced etching rate resulting from the laser exposure is driven by two phenomena: The first one being the SiO₂ matrix modifications induced in the laser spot which promotes the etching rate by forming lower-size rings with smaller bond angles; and the second one being the stress resulting from these modifications. The two effects appear to be cumulative. If the stress around the LAZ is removed (for instance due to stress-relaxation mechanisms), structural modifications in the LAZ is still present and locally enhances the etching rate. This effect could possibly explain why, passed a maximum value, corresponding to a maximized stress-induced effects, the etching rate does not drop down to zero but continues at a same pace.

5. Conclusion

We have found that the net deposited energy plays a key role in deciding the etching rate of laser processed bulk fused silica. There is an optimum deposited energy to achieve maximum etch rate. In other words we have identified a clear way to select appropriate parameters for fast micromachining in fused silica which is very significant from the industrial point of view. We demonstrate that a writing speed of even 30 mm/s is possible and may be even higher by modifying the laser writing set up. The present results further support the densification based model of femtosecond laser-fused silica interaction.

Acknowledgments

The authors acknowledge the financial support from the European Commission under the 6th Framework Programme (GOLEM, NMP, 033211) and the Excellentie Funds of Eindhoven University of Technology (Yves Bellouard).